Journal of Thermal Analysis and Calorimetry (2019) 135:2613–2623
https://doi.org/10.1007/s10973-018-7334-4

Co-pyrolysis and catalytic co-pyrolysis of *Enteromorpha clathrata* and rice husk

Toward high-quality products

Shuang Wang[1] · Bin Cao[1] · Yongqiang Feng[1] · Chaoqun Sun[1] · Qian Wang[1] · Abd El-Fatah Abomohra[1,2] · Stephen Afonaa-Mensah[1] · Zhixia He[1,3] · Bo Zhang[3] · Lili Qian[1] · Lujiang Xu[4]

Received: 30 December 2017 / Accepted: 24 April 2018 / Published online: 8 May 2018

Abstract
Catalytic co-pyrolysis process of *Enteromorpha clathrata* (EN) and rice husk (HU) was studied in a fixed bed reactor with ZSM-5 and MCM-41 catalysts at 550 °C. The yields and product distribution were compared when EN, HU and different mass ratios of EN and HU were pyrolyzed with or without catalysts. Bio-oil products were analyzed by Fourier transform infrared spectroscopy and gas chromatography-mass spectrometry (GC–MS) and bio-char products were analyzed by X-ray photoelectron spectroscopy. Under co-pyrolysis conditions without catalysts, the experimental yield of bio-gas was higher than the theoretical. In contrast, the yield of bio-oil was lower than the theoretical. In the catalytic pyrolysis, ZSM-5 significantly improved the yield of bio-oil and reduced the bio-gas product. However, the effect of MCM-41 on the yield of the pyrolysis products was weaker than that of ZSM-5. In the GC–MS analysis of bio-oil with catalysts, ZSM-5 showed a catalytic effect on the decomposition of hemicellulose and protein. The protein was further cracked, and the relative content of hydrocarbon component also increased. With MCM-41 catalyst, there was significant catalytic effect on lignin and lipid, and the result showed that MCM-41 had a further catalytic influence in the synergetic effect of co-pyrolysis.

Keywords Catalytic co-pyrolysis · *Enteromorpha clathrata* · Rice husk · Zeolite · GC–MS

Introduction

Biomass is an abundant, carbon neutral and renewable substitute for fossil fuels, which has a potential to alleviate the energy crisis [1]. In the last decades, different types of biomass have been investigated such as rice husk, pine-wood, oak, white pine, scum, sorghum bagasse [2–4], and so on. Currently, the utilization of algae has drawn considerable attention due to its various advantages. For example, algae have higher growth rate, shorter growth cycle and do not compete in land use for food production. In addition, productivity of some algae can be as high as that of most productive terrestrial biomass. Another advantage of algae is the high metal (K, Na) concentrations. Although alkali metal may lead to decrease in bio-oil yield, it can have a catalytic effect on conversion processes to obtain high-quality bio-oil [5].

Pyrolysis is one of the most important conversion approaches of biomass. Through the pyrolysis, the biomass structure components decompose to lower molecular weight products such as bio-gas, bio-oil, bio-char products and other platform chemicals. There are many studies on the pyrolysis of terrestrial biomass and algae biomass. Hemicellulose, cellulose and lignin form the structure of the terrestrial biomass, while algae biomass consists of

✉ Lujiang Xu
lujiangxu@njau.edu.cn

[1] School of Energy and Power Engineering, Jiangsu University, Zhenjiang 212013, Jiangsu, China

[2] Botany Department, Faculty of Science, Tanta University, Tanta 31527, Egypt

[3] Institute for Energy Research, Jiangsu University, Zhenjiang 212013, Jiangsu, China

[4] College of Engineering, Nanjing Agricultural University, Nanjing 210031, Jiangsu, China

three main components, namely proteins, polysaccharides and lipids. The co-pyrolysis of algae and terrestrial biomass has certain synergetic effects on the products [6]. Hua et al. investigated the co-pyrolysis characteristics of the sugarcane bagasse and *Enteromorpha prolifera* in a fixed bed reactor. The results showed that the acidity and density of bio-oils decreased and the calorific value increased through the co-pyrolysis [7]. Li et al. [8] found that co-pyrolysis tar of rice straw and Shenfu bituminous coal contained more phenolics, less oxygenate compounds and higher gas yields. Alvarez et al. [9] investigated co-pyrolysis of sewage sludge and lignocellulosic biomass in a conical spouted bed reactor, which showed that gas product increased significantly.

However, it should be noted that bio-oil is not economically at present. It has been observed that there are many oxygenates in the liquid product. This leads to some negative properties about their chemical and physical characteristics, such as high acidity, oxygen content, high density and so on [10–12]. Several methods have been therefore utilized to upgrade the quality of bio-oil. Catalytic pyrolysis is one of effective methods to deoxygenate and promote the cracking reactions of large molecules during the pyrolysis. Zeolite catalysts at atmospheric pressure have been used to produce high-quality bio-oil and eliminate the secondary reactions of bio-oil. Zeolite catalysts have received much attention and been widely investigated by several researchers [13–17]. There are extensive evidences that ZSM-5, as one kind of acidic and porous zeolite, is an adaptive catalyst for pyrolysis of biomass. Wang et al. presented an investigation into the catalytic cracking of pinewood pyrolysis with HZSM-5 at different temperatures. The results showed that HZSM-5 could promote decarbonylation and decarboxylation with inhibited dehydration [18]. Chiara Lorenzetti et al. studied the upgrading of pyrolysis oil obtained from lignocellulosic and proteinaceous over HZSM5, which exhibited a significant dehydration, deoxygenation, denitrogenation effect. It also induced the formation of nitrogen-containing polyaromatic compounds [19]. Aiming Zheng et al. reported that catalytic pyrolysis of different biomass species over ZSM-5 with varying crystal size can promote the formation of aromatic [20].

In this work, *Enteromorpha clathrate* (EN) and rice husk (HU) were selected as representative materials of algae and agricultural wastes. A fixed bed reactor was used to investigate the performance of ZSM-5 and MCM-41 catalyst on catalytic co-pyrolysis of EN and HU. The first objective in this study was to investigate the synergetic effects in the co-pyrolysis of algae and terrestrial biomass. The second objective was to investigate the impact of ZSM-5 and MCM-41 on the co-pyrolysis of EN and HU. Fourier transform infrared spectroscopy (FTIR) and gas chromatography-mass spectrometry (GC–MS) were used to analyze the chemical compositions of bio-oils, which aimed to further investigate the effects of co-pyrolysis and catalysts on the product yields and composition distribution of bio-oil. In addition, X-ray photoelectron spectroscopy (XPS) measurements of the chars have been performed.

Our previous work showed that there was a synergistic interaction for the co-pyrolysis of *Enteromorpha clathrata* and rice husk from TG-FTIR-MS analysis [21]. Based on the previous work, the present work has three points of significance as following:

1. *Enteromorpha clathrate* (EN) and rice husk (HU), as representative materials of algae and agricultural wastes, respectively, will be selected for the co-pyrolysis and catalytic co-pyrolysis toward high-quality products. This provides the reference for the utilization of algae and agricultural wastes.
2. The present work will also give an insight into the effect for the co-pyrolysis of *Enteromorpha clathrata* and rice husk on the component distribution of bio-oil in detail. The effect of different mass ratios of *Enteromorpha clathrata* and rice husk on the product yields will also be studied to disclosed the effect of mass ratio on the synergistic interaction.
3. The present work will provide the reference for the selection of catalyst to produce high-quality bio-oils based on the component analysis of bio-oils in the co-pyrolysis of algae and agricultural wastes.

Materials and methods

Materials

EN and HU used for this study were collected from Xiangshan Port, Zhejiang Province and Huai'an, Jiangsu Province in China, respectively. The proximate analysis of the two-biomass samples is shown in Table 1. The samples were first ground by mill cut and then sieved to a particle size smaller than 0.18 mm, and they were pre-dried at 105 °C for 4 h. Dried EN and HU were mixed together at ratios of 1:1, 1:2, 1:3, 2:1, and 3:1, respectively.

Table 1 Proximate analysis of EN and HU

Sample	Proximate analysis/%			
	M_{ad}	A_{ad}	V_{ad}	FC_{ad}
EN	9.358	29.312	55.731	5.599
HU	12.652	11.808	68.139	7.401

Catalysts

ZSM-5 (SiO_2/Al_2O_2 = 36 and surface area = 350 $m^2\ g^{-1}$) and MCM-41 (SiO_2/Al_2O_2 = All-silicon and surface area = 1180 $m^2\ g^{-1}$) catalysts were purchased from Nankai University Catalyst Co., Ltd. MCM-41 was activated in a muffle furnace at 120, 250, 350, 550 °C for 2 h, respectively.

Pyrolysis experiment

The test of catalytic co-pyrolysis of EN and HU was carried out in a fixed bed reactor (height: 100 mm, internal diameter: 70 mm). The experiment system is shown in Fig. 1. In a typical run, the preheating temperature was 500 °C, and the reactor was heated up to the end temperature of 550 °C at N_2 flow of 200 mL min^{-1}. After that, 5 g dried sample was put into the reactor for a retention time of 20 min. The samples decomposed to produce biochar, bio-oil and bio-gas. The pyrolysis gas passed though the condensation unit was collected as bio-oil, while the non-condensable gas was collected in gas collecting bags.

Product analysis

The bio-oil products required pretreatment of dehydration and filtration by anhydrous sodium sulfate and organic filters. The samples were analyzed on a gas chromatograph (Agilent, 7890A) couple with a mass spectrometer (Agilent, 5975C), equipped with a non-polar column (HP-5MS). The carrier gas (Helium) flow rate was 1 mL min^{-1}, and the split ratio was 5:1. The temperature of injector was set at 250 °C. Solvent delay time was 5 min, and the full-scan mode with mass to charge ratios of 12–500 was used. The GC oven temperature program was 60 °C for 2 min, and ramped to 120 °C at a heating rate of 10 °C min^{-1} where it was held for an additional 2 min, then reached up to 200 at 4 °C min^{-1}, holding for 2 min, finally up to 260 at 5 °C min^{-1}. The chemical compounds in the bio-oil were identified by the National Institute of Standards and Technology (NIST) mass spectral library. The infrared spectrum of the bio-oil was determined using Nicolet Nexus 470 FTIR Spectrometer. A 32-scan adsorption interferogram was collected at a 2 cm^{-1} resolution in the 4000–500 cm^{-1} region at room temperature. X-ray photoelectron spectroscopy (XPS) measurements of the chars were performed in the Thermo Fisher Scientific, ESCALAB250Xi.

Yields of products

The yields of bio-oil, bio-char and bio-gas products from the experiments were calculated by the following equations:

$$\text{Bio-oil product yield}: W_1 = \frac{M_1}{M_0} \times 100\% \quad (1)$$

$$\text{Bio-char product yield}: W_2 = \frac{M_2}{M_0} \times 100\% \quad (2)$$

$$\text{Bio-gas product yield}: W_3 = 100\% - W_1 - W_2 \quad (3)$$

To investigate the synergetic effects in the catalytic co-pyrolysis of EN and HU, the theoretical value of the pyrolysis products was calculated by the following equation:

$$Y_{\text{Theoretical}} = \omega \times Y_{\text{EN}} + (1 - \omega) \times Y_{\text{HU}} \quad (4)$$

where Y_{EN}, Y_{HU} and $Y_{\text{Theoretical}}$ are the experimental value of two kinds of materials and their theoretical mass average value; ω represents the percentage mass of EN in the mixed samples.

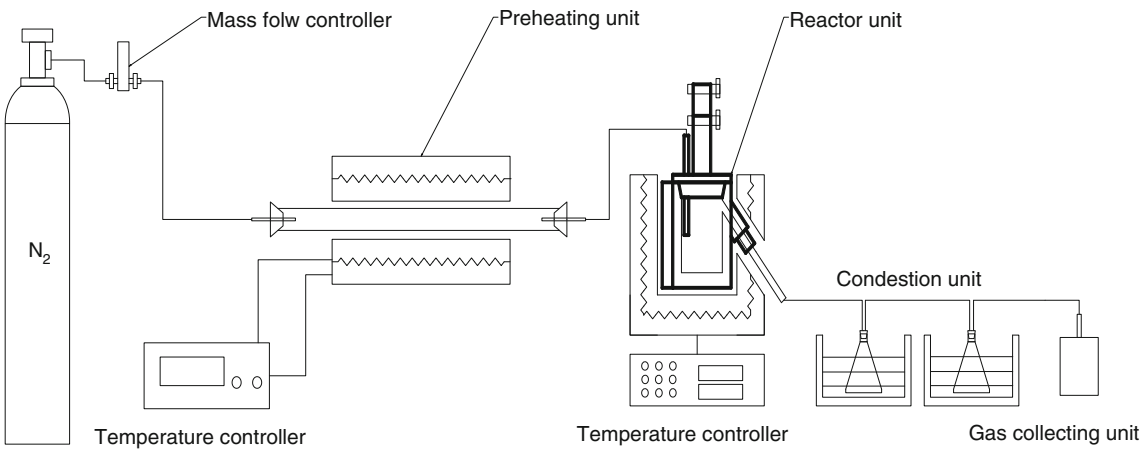

Fig. 1 Schematic diagram of the pyrolysis system

Results and discussion

Co-pyrolysis experiment

Product yields of the co-pyrolysis

The yields of bio-oil, bio-char, and bio-gas in co-pyrolysis of different mass ratio of EN and HU at 550 °C are shown in Fig. 2. The repeatability examinations for the analytical pyrolysis experiments revealed that the relative errors of the product yields were generally within ± 5%. The yields of bio-oil, bio-char, and bio-gas products were 29.56, 46.76, and 23.68%, respectively, when the pyrolysis material was only EN, while those were 40.26, 34.39, and 25.35% for only HU. In contrast, the bio-oil yield of EN was 10.70% lower than that of HU, and the solid yield was 12.37% higher than that of HU. This was attributed to the ash content of the biomass sample. From Table 1, the ash content of EN was 29.31%, which was higher than that of HU, while the volatile content of EN was lower than that of HU. In addition, there were more alkali metals in the ash content of EN in the form of oxides and chlorides. Na and K content in the ash of EN was 18.28 and 12.70%, respectively [22]. Studies had shown that alkali metal elements had certain catalytic effects on the pyrolysis reactions. In the co-pyrolysis, adding alkali metal catalysis (Na, K) could reduce the pyrolysis temperature, promote the cracking reactions of the molecules and improve the gas product [23].

According to Eq. (4), supposing that there is no interaction between EN and HU, the theoretically calculated product yields with different mass ratios of EN and HU of 3:1, 2:1, 1:1. 1:2, 1:3 were determined and compared with experiment results in Fig. 2. The experimental yields of bio-oil for each mass ratio were all lower than the theoretical values. The maximum difference between the experimental and the theoretical was up to 5.91% when the mass ratio was 1:1. However, the experimental yields of bio-gas were significantly higher than the theoretical. Maximum difference up to 5.90% was observed at 1:1 mass ratio. This result indicated that there was a synergetic effect during the co-pyrolysis between EN and HU, which could promote the secondary cracking reactions, resulting in more bio-gas which was cracked from macromolecules. The yield of bio-oil decreased and that of bio-gas increased. However, the experimental yields of solid products were consistent with the theoretical ones. Due to the most remarkable synergetic effect on the yields of bio-oil and bio-gas during the co-pyrolysis between EN and HU with mass ratio of 1:1, the catalytic pyrolysis experiments were conducted with the mass ratio of EN and HU of 1:1.

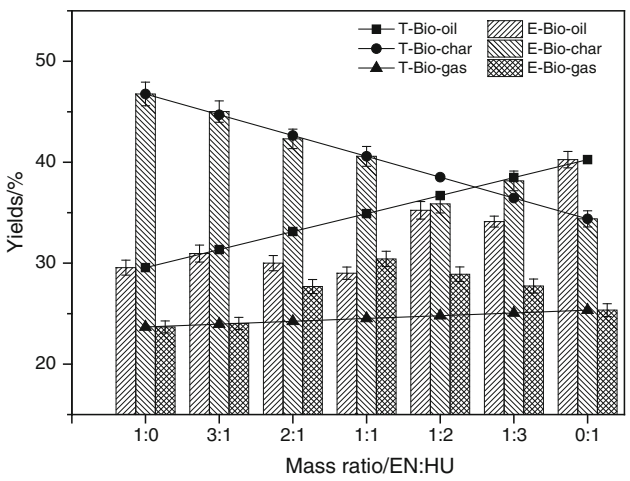

Fig. 2 Yields of liquid, solid and gas productions in co-pyrolysis

GC–MS analysis of co-pyrolysis bio-oil

In order to further investigate the synergistic effect of co-pyrolysis, GC–MS analysis of bio-oil was carried out in this study. There were a variety of organic compounds in the bio-oil. According to GC–MS analysis, the organic compounds were classified into several groups: phenols, acids, alkanes, aldehydes, ketones, alcohols, esters, pyridines, furan, imidazole and the other substances. The results showed that there were many acid compounds in pyrolysis bio-oil of EN, which were mainly formic acid and acetic acid. The relative contents of hydrocarbons, esters, phenols, aldehydes and ketones were also high, while there were only small percentages of heterocyclic compounds, furan derivatives, pyridine, and imidazole nitrogen derivatives. For bio-oil from EN, there were a lot of phenol compounds, whose content reached up to 28.50%, and the acid content was 17.52%, lower than that of HU. Compared to the bio-oil from HU, there were more furans but lower nitrogenous compounds in the bio-oil from EN. The main reason was that the main components of EN were proteins, polysaccharides and lipids. Pyridine, imidazole and the other nitrogenous heterocyclic derivatives compounds in bio-oil of EN were related to the decomposition of proteins and the Maillard reaction of amino acids with carbohydrates [24]. The main components of HU were lignocellulose. Furans and phenols were the typical products of cellulose and lignin pyrolysis [25].

Figure 3 shows the compounds distribution of co-pyrolysis bio-oil. According to the Eq. (4), theoretical values of the compounds distribution were calculated using the experiment results when EN and HU were pyrolysis alone. The relative contents of acids in the bio-oil from the co-pyrolysis increased. Maximum of 47.60% was observed at mass ratio of 3:1, exceeding the theoretical relative content of 20.04%. The acids in the bio-oil were mainly acetic acid,

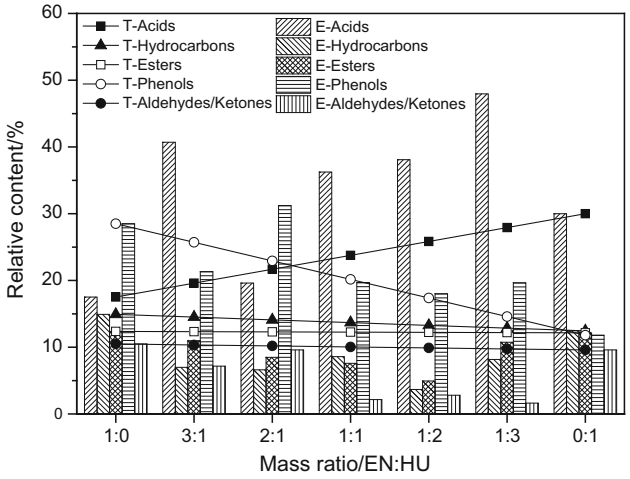

Fig. 3 Bio-oil composition in co-pyrolysis of different blending ratios

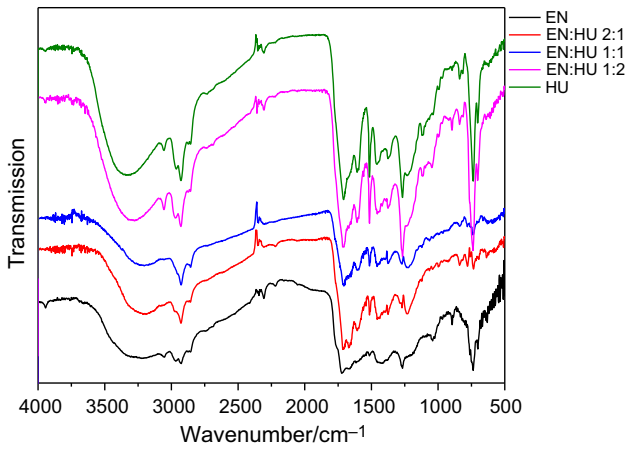

Fig. 4 TFIR profiles of co-pyrolysis at different blending ratio

palmitic acid, propionic acid and propylene acid. The relative content of palmitic acid in the bio-oil from co-pyrolysis decreased, which that of acetic acid increased significantly. At the same time, the relative content of esters, aldehydes and ketones in the co-pyrolysis bio-oil was lower than that of the corresponding theoretical values. However, there was little difference between the theoretical and experimental values of phenolic compounds. This means that the synergetic effect of the co-pyrolysis promoted the formation of small molecular acid and reduced the selectivity of aldehydes, ketones and esters. However, there were no significant impacts on phenolic compounds.

In the lignocellulose biomass pyrolysis process, acetic acid was mainly derived from small molecular compounds generated by the breaking of hemicellulose-rich branched chain [26]. The content of ash was high in EN, which contained a lot of alkali metal elements, such as K and Na. It could be speculated that Na and K elements had a significant effect on the formation of small molecular components in the lignocellulosic biomass pyrolysis products [27], resulting in the increase in smaller molecular compounds in the co-pyrolysis of the EN and HU. Co-pyrolysis promoted the selectivity of acetic acids in small molecules. Acetic acid, furfural and phenol in bio-oil were high value-added chemical products. The use of existing extraction technology to extract high value-added chemical products of bio-oil had a broad prospect.

FTIR analysis of co-pyrolysis bio-oil

Figure 4 shows the spectra of the co-pyrolysis bio-oil from the FTIR analysis. The C=O stretching vibration was observed at the peak range from 1705 to 1725 cm^{-1}, and the band at 1220–1270 cm^{-1} and 3250–3330 cm^{-1} was characteristics of C–O and O–H groups, which proved the existence of the carboxylic acid.

The C-H bending vibration that was observed at the peak ranged from 730 cm^{-1} to 745 cm^{-1}, and the O–H bending vibration in the range of 3250–3330 cm^{-1} was identified as phenol, which was typical products from the pyrolysis of cellulose. Besides that, the peak at 2920–2930 cm^{-1} was assigned to stretching vibration of C–H, and the peak at 730–745 cm^{-1} was assigned to out-of-plane bending vibration of C–H. The analysis results were consistent with compounds observed by GC–MS.

XPS analysis of co-pyrolysis bio-char

Figure 5 shows the C1*s* and N1*s* spectra of bio-char from EN, EN + HU (1:1), and HU at the temperature of 550 °C. The bio-chars of EN, EN + HU (1:1), and HU at the temperature of 550 °C were marked as Y1, Y2 and Y3, respectively. XPS analysis of the carbon-containing and nitrogen-containing functional groups is shown in Table 2. The C1*s* spectrum of bio-chars comprised four peaks at (284.6 ± 0.3) eV, (286.1 ± 0.3) eV, (287.6 ± 0.3) eV, and (289.1 ± 0.3) eV, corresponding to: aliphatic carbon C–C/C=C/C-H groups (C1), C–O/C–O–C groups in alcohol, ether groups (C2), C=O groups in carbonyl groups (C3) and COO– groups in carboxyl and/or ester groups (C4), respectively [28–30]. Comparing Y2 and Y2-T, the content of COO– groups for Y2 was lower than that of Y2-T, which indicated that there was some kind of synergetic effect of transferring COO– groups in bio-chars into bio-oils during the co-pyrolysis of EN and HU. This result was consistent with that in GC–MS analysis (Fig. 3).

The binding energies at (398.7 ± 0.4) eV, (400.4) eV and (401.1 ± 0.3) eV in the N1 s spectrum were assigned to the *N* in the pyridine nitrogen, protein nitrogen, and ammonium nitrogen [28, 31, 32]. During co-pyrolysis of

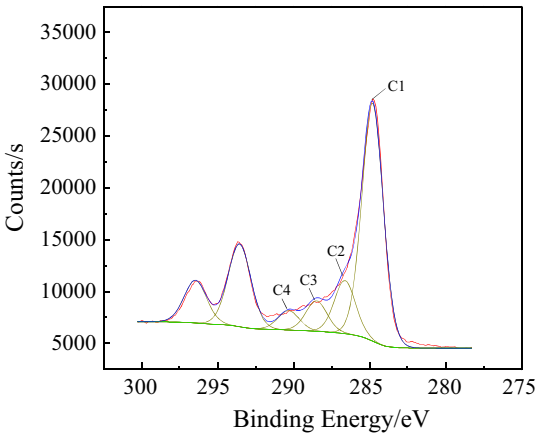

EN 550 °C C1*s* spectra

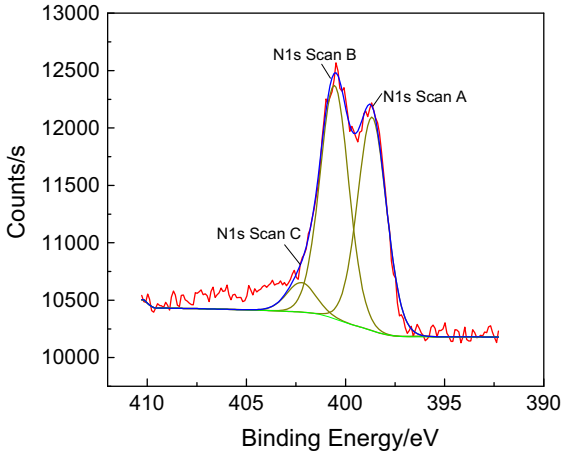

EN 550 °C N1*s* spectra

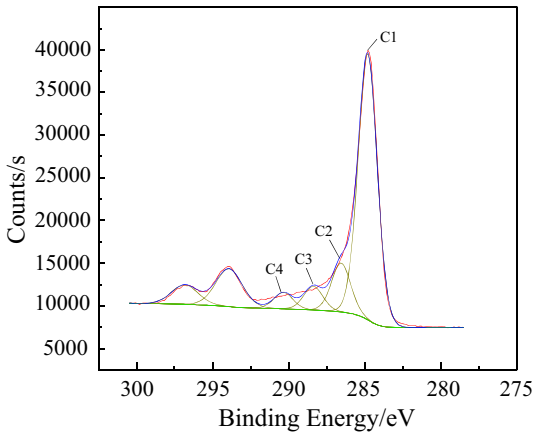

EN+HU 550 °C C1*s* spectra

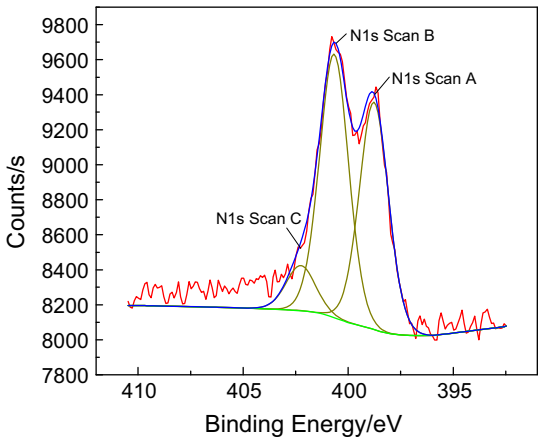

EN+HU 550 °C N1*s* spectra

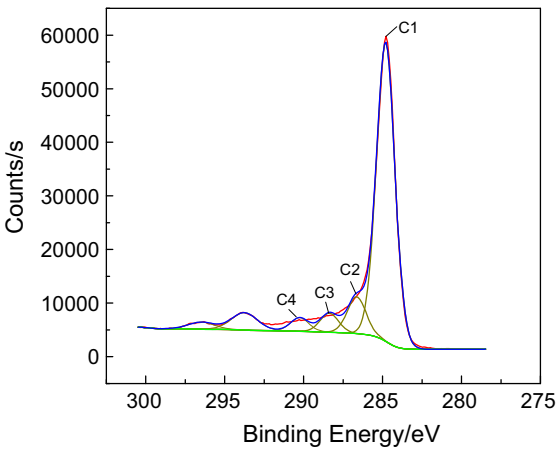

HU 550 °C C1*s* spectra

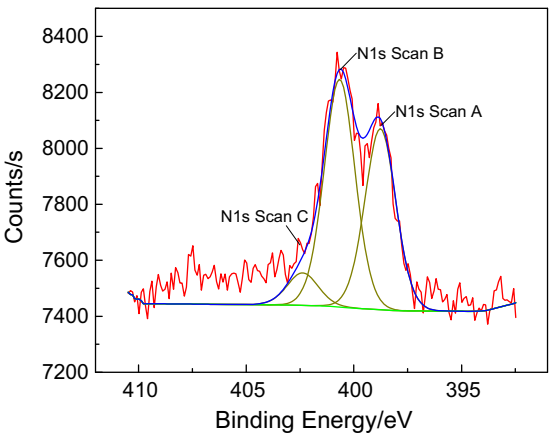

HU 550 °C N1*s* spectra

Fig. 5 The C1*s* and N1*s* spectra of bio-char samples

Table 2 XPS results of carbon and nitrogen forms and their contents

	E/eV	C/O/N forms	Content/%			
			*Y*1	*Y*2	*Y*2-*T*	*Y*3
C1	284.6	C–C/C=C/C–H	69.9	75.0	75.5	81.1
C2	286.1	C–O/C–O–C	15.6	13.8	12.8	10.0
C3	287.6	C=O	8.8	6.6	6.95	5.1
C4	289.1	COO–	5.7	4.6	4.75	3.8
N1	398.7	Pyridine-*N*	44.8	42.4	42.9	41.0
N2	400.4	Protein-*N*	49.0	49.2	50.3	51.6
N3	401.1	Ammonium-*N*	6.2	8.4	6.8	7.4

*Y*2-*T* = (*Y*1 + *Y*3)/2: the theoretical value of *Y*2.

EN and HU, the contents of pyridine-*N*, protein-*N* and ammonium-*N* in experiments were 42.4, 49.2 and 8.4%, while those of theoretical values were 42.9, 50.3 and 6.8%, respectively. The contents of pyridine-*N* and protein-*N* in experiments were lower than those of pyridine-*N* and protein-*N* of theoretical value, while the content of ammonium-*N* in the experiment was higher than that of ammonium-*N* of theoretical value. Pyridine-*N* was mainly derived from the deamination or dehydrogenation of amino acids, while ammonium-*N* mainly resulted from the conversion of pyridine-*N* [31, 32]. Furthermore, pyridine-*N* might be converted into more stable ammonium-*N* [32]. This could be the possible reason that the content of ammonium-*N* in experiment was higher than that of theoretical value during the co-pyrolysis of EN and HU. The experimental values of C=O and protein-*N* were 6.6 and 6.95%, while the theoretical values of C=O and protein-*N* were 49.2 and 50.3%. The experimental values were slightly lower than theoretical ones, which might be ascribed to Maillard reaction through which some amino acids (protein-*N*) reacted with carbonyl groups (C=O) during co-pyrolysis of EN and HU, reducing the contents of carbonyl groups and protein-*N*.

Catalytic co-pyrolysis experiment

The ZSM-5 and MCM-41 catalysts were used in the catalytic pyrolysis experiments, both of which are zeolite catalysts. The ZSM-5 is micropores acid catalysts, which has received widespread attention. ZSM-5 has a small pore size, high acidity, moderate internal pore space and steric hindrance. By contrast, MCM-41 is mesoporous catalysts and its acidity is weaker than that of ZSM-5.

Product distributions during the catalytic co-pyrolysis

Table 3 shows the product distribution in catalytic co-pyrolysis of EN and HU with different catalysts. The mass ratio of biomass to catalyst was 10:1, and the reaction temperature was 550 °C. As shown in Table 3, the yield of bio-oil increased significantly under ZSM-5 catalysts compared to non-catalytic pyrolysis while that of gas decreased for the EN and HU pyrolysis. The yield of bio-oil increased by 7.95 and 8.98% for EN and HU, respectively. However, MCM-41 catalyst had different catalytic effects on the EN and HU. For EN, the bio-oil yield increased by 3.8% with the MCM-41 catalyst, which was similar to that of ZSM-5, but it was not significant. The catalytic effect of MCM-41 on the product yields of HU was weak. Possible reason was that ZSM-5 had

Table 3 The yield distribution in the pyrolysis experiments with or without catalysts

Sample	Catalyst	Bio-oil/%	Bio-char/%	Bio-gas/%
EN	Non-catalyst	29.56	46.76	23.68
	ZSM-5	37.51	44.90	17.59
	MCM-41	33.36	48.54	18.10
HU	Non-catalyst	40.26	34.39	25.35
	ZSM-5	49.24	34.40	16.36
	MCM-41	39.52	35.29	25.19
EN: HU = 1: 1	Non-catalyst	29.00	40.58	30.42
	ZSM-5	38.66	38.10	23.24
	MCM-41	34.52	42.38	23.09
	ZSM-5: MCM-41 = 1: 1	34.71	43.25	22.03

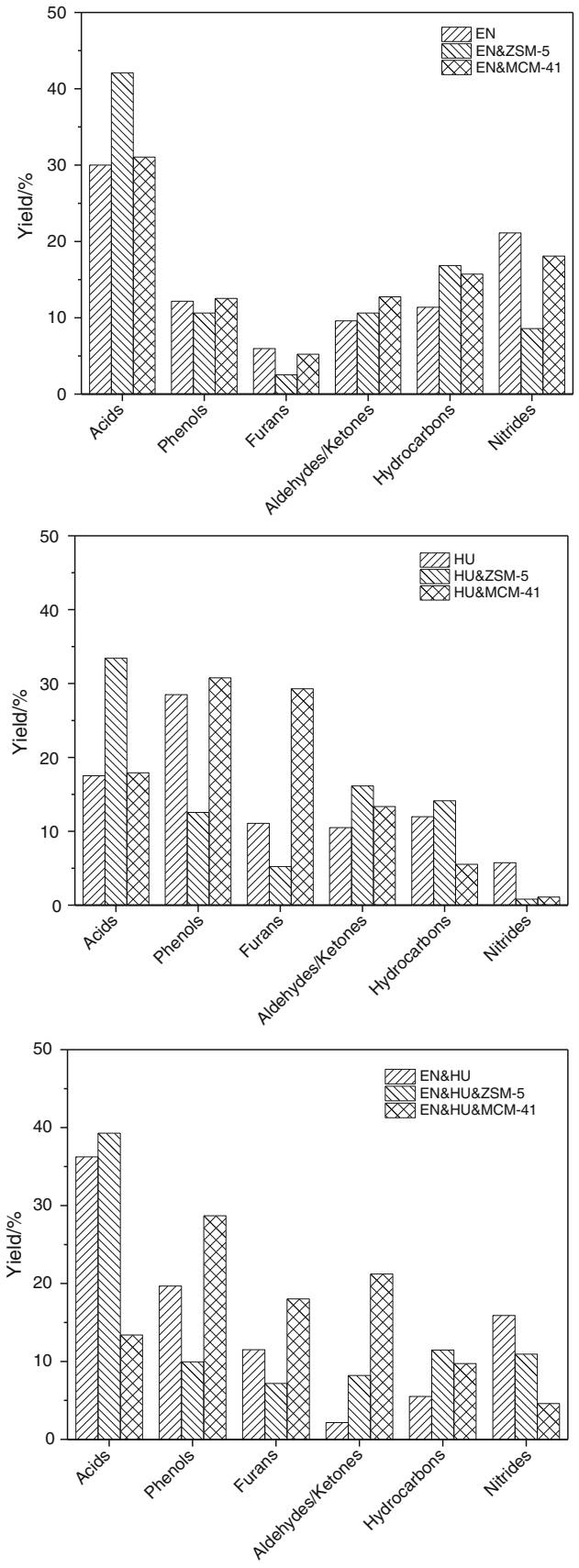

Fig. 6 Bio-oil composition in catalytic pyrolysis of EN and HU

suitable internal pore space and steric hindrance that favored catalytic pyrolysis of biomass than MCM-41 for EN and HU pyrolysis.

In the catalytic co-pyrolysis experiments, the effects of the catalysts on the product yield were basically consistent with the expected results of the EN and HU catalytic pyrolysis alone. The yield of co-pyrolysis bio-oil increased by 9.66 and 2.52% with ZSM-5 and MCM-41 catalysts, respectively. However, the bio-gas yield decreased to 22.03% with the combination of ZSM-5 and MCM-41, corresponding to the increase in bio-char yield. It indicated that the combination of ZSM-5 and MCM-41 catalysts promoted the formation of bio-char, hence reducing the bio-gas yield.

GC–MS analysis of catalytic co-pyrolysis bio-oil

The main chemical species in catalytic co-pyrolysis bio-oil analyzed using GC–MS were grouped into five categories (acids, phenols, furans, aldehydes and ketones, and hydrocarbons), as shown in Fig. 6. The presence of catalysts had obvious influences on the product quality and distribution. Acids and phenols were the principal components for the bio-oil in the catalytic pyrolysis of EN and HU. Acids were the main pyrolysis products of hemicellulose and protein [33]. It could be found that the ZSM-5 catalyst promoted the formation of acid compounds and furan while suppressed *N*-containing compounds. Furans are the main products of cellulose and hemicellulose, while *N*-containing compounds are mainly derived from the pyrolysis of protein [20]. This further indicated that ZSM-5 has a significant catalytic effect on the protein and hemicellulose, enhanced the selectivity of acids compounds, and therefore reduced the formation of furans compounds, and promoted the decomposition of protein.

The phenols components in bio-oil from the pyrolysis of HU reached up to 28.5%. This is because phenol, as the representative component of the phenolic, was an important product from the pyrolysis of lignin. In the catalytic pyrolysis products, MCM-41 showed obvious selectivity to phenolic compounds [34], whose relative content in bio-oil from the pyrolysis of HU reached up to 30.77%, while that of ZSM-5 was only 11.46%. The pore size of the hierarchical mesoporous zeolite catalysts played a pivotal role as it reckoned the bio-oil speciation and distribution of the pyrolysis products.

With the MCM-41 catalyst, the proportion of furans in pyrolysis bio-oil of EN did not change that much, but the furan content of HU increased obviously. In addition, the acids in pyrolysis bio-oil of EN and HU as a typical hemicellulose and protein pyrolysis products did not change significantly with catalyst. This indicated that MCM-41 had a significant catalytic effect on cellulose.

Table 4 The main components of bio-oil in catalytic experiments

Compounds	Relative contents/%							Molecular weight
	EN		HU		EN and HU			
	ZSM-5	MCM-41	ZSM-5	MCM-41	ZSM-5	MCM-41	ZSM-5&MCM-41	
Acetic acid	18.46	4.70	21.59	9.74	21.16	8.19	8.76	60.021
n-Hexadecanoic acid	13.38	18.20	–	3.82	4.83	11.16	3.35	256.24
Phenol	6.54	4.06	5.47	5.68	4.50	4.44	7.70	94.042
Propanoic acid	5.39	2.67	11.18	3.25	3.82	2.46	3.45	74.037
2-Furancarboxaldehyde, 5-methyl	2.52	3.48	–	2.31	1.83	10.71	10.46	110.037
Benzofuran, 2,3-dihydro	–	–	5.23	5.08	5.34	6.90	6.69	120.058
Phenol, 4-methyl	4.09	4.78	1.99	4.49	2.03	3.64	7.27	108.058
2-Cyclopenten-one, 2-methyl	–	10.14	3.90	3.05	–	2.40	4.81	96.058
Phenol, 2-methoxy	–	–	3.26%	6.51	3.41	3.86	3.56	124.052
2-Propenoic acid	4.87	5.49	–	–	3.46	2.11	2.00	72.021
Furan, 2-methyl	–	1.76	–	3.71	2.39	3.13	4.39	82.042
1,2-Cyclopentanedione, 3-methyl	2.38	2.39	–	3.01	–	3.07	3.03	112.052
1-Hydroxy-2-butanone	–	–	3.99	3.00	3.03	0.69	1.18	88.052

"–" Means not detected

Additionally, in the catalytic co-pyrolysis of EN and HU, the acid compounds decreased to 13.39% while the relative content of ketone significantly increased with the MCM-41 catalyst. This result suggested that the synergistic effect of co-pyrolysis had an influence on the catalysis and promoted the dehydration reaction. As mentioned above, the bio-oil compositions produced from the catalytic co-pyrolysis had a strong connection with the structural composition of the biomass and the type of catalyst.

Figure 6 shows the mainly compounds in the bio-oils obtained from catalytic co-pyrolysis of EN and HU. Acidic components were mostly derived from hemicellulose and protein cracking, and the cracking of cellulose and algae polysaccharide also had a small amount of acid products. In the acid component, acetic acid, propionic acid, propenoic acid and hexadecanoic acid were common products. Acetic acid is most easily produced from pyrolysis, while propionic acid is mostly derived from the oxidation of propanal. Hexadecanoic acid is a macromolecule, a product of lipid pyrolysis. ZSM-5 showed a strong selectivity to acetic acid, and with ZSM-5 catalysis, the content of acetic acid in EN and HU pyrolysis bio-oil reached up to 18.46 and 21.59%, respectively. Acetic acid is mostly derived from the break of rich branch of xylan in hemicellulose, which further illustrated the selective catalytic effect of ZSM-5 on xylan. Besides that, the content of hexadecanoic acid was higher with MCM-41 catalyst than ZSM-5, which suggested that MCM-41 had greater effects on the pyrolysis of lipids in algae than ZSM-5.

During the catalytic pyrolysis, bio-char was deposited on the catalyst surface. The study has shown that bio-char was the product of furan polymerization. The furan stimulated higher coking compared to the other derivatives [35]. As shown in Fig. 6, the trend of bio-char was similar to that of the relative content of furans. From Table 4, the relative content of 5-methyl-2-furancarboxaldehyde ($C_6H_6O_2$) was significantly changed under different conditions. Furfural ($C_5H_4O_2$) was produced by the cracking of cellulose, hemicellulose and algae polysaccharides. Cellulose and algae polysaccharides were hexoses, requiring cracking reactions to obtain furfural. Hemicellulose, as pentoses, did not need to crack to produce furfural; thus, the furfural had a different generation path. The relative contents of 5-methyl-2-furancarboxaldehyde ($C_6H_6O_2$) with MCM-41 catalyst were higher than those with ZSM-5. The highest relative content reached up to 10.71%. MCM-41 promoted the selectivity of furfural ($C_5H_4O_2$) components and had further catalytic characteristics under the synergistic effect of co-pyrolysis, which obviously promoted the formation of 5-methyl-2-furancarboxaldehyde ($C_6H_6O_2$). The main reason was that the MCM-41 had a larger pore size, which allowed the oligomers of protein and carbohydrate to break into the microporous molecular sieves and undergo secondary cleavage.

Conclusions

From the analysis of the three-phase product yields obtained from co-pyrolysis of EN and HU, the yield of biogas product was obviously higher than the theoretical value. In contrast, the experimental yield of bio-oil product

was lower than the theoretical, while the experimental yield of bio-char was consistent with the theoretical. Considering the bio-oil from co-pyrolysis of EN and HU, the small molecular acid in the experiment was obviously higher than that of the theoretical. The increase in bio-gas product proved that alkali metal elements (Na, K) in EN ash promoted the further cracking of macromolecules into small molecules during the pyrolysis process.

In the catalytic pyrolysis, ZMS-5 significantly improved the yields of bio-oil while it reduced the bio-gas product. However, the effect of MCM-41 on the yields of the pyrolysis products was weaker than those of ZSM-5. The catalytic pyrolysis bio-oil yield of EN increased slightly, while that of HU did not change too much with MCM-41 catalyst. This indicated that ZSM-5 had a higher catalytic effect than MCM-41 in terms of yield. In the GC–MS analysis of catalytic pyrolysis bio-oil, the main components were acids, phenols and furan products. The effect of ZSM-5 on the pyrolysis of hemicellulose and protein was that the relative content of acids in bio-oil increased significantly. In addition, the protein was further cracked to the nitrogen-containing components and the relative content of hydrocarbon component also increased. With the MCM-41 catalyst, the contents of phenolic components and hexadecanoic acid increased. Besides that, the content of 5-methyl-2-furancarboxaldehyde also showed a significant increase. All the results showed that MCM-41 had a further catalytic influence in the synergetic effect of co-pyrolysis. The results provided the reference for the selection of mass ratio and catalyst to produce high-quality bio-oils in the co-pyrolysis of algae and agricultural wastes.

Acknowledgements This work was supported by the National Natural Science Foundation of China [grant numbers 51676091].

References

1. Suutari M, Leskinen E, Fagerstedt K, Kuparinen J, Kuuppo P, Blomster J. Macroalgae in biofuel production. Phycol Res. 2015;63(1):1–18. https://doi.org/10.1111/pre.12078.
2. Kotaiah Naik D, Monika K, Prabhakar S, Parthasarathy R, Satyavathi B. Pyrolysis of sorghum bagasse biomass into bio-char and bio-oil products. J Therm Anal Calorim. 2017;127(2):1277–89. https://doi.org/10.1007/s10973-016-6061-y.
3. Wang X, Wang X, Qin G, Chen M, Wang J. Comparative study on pyrolysis characteristics and kinetics of lignocellulosic biomass and seaweed. J Therm Anal Calorim. 2018;132(2):1317–23. https://doi.org/10.1007/s10973-018-6987-3.
4. Quan C, Xu S, An Y, Liu X. Co-pyrolysis of biomass and coal blend by TG and in a free fall reactor. J Therm Anal Calorim. 2014;117(2):817–23. https://doi.org/10.1007/s10973-014-3774-7.
5. Mourant D, Wang Z, He M, Wang XS, Garcia-Perez M, Ling K, et al. Mallee wood fast pyrolysis: effects of alkali and alkaline earth metallic species on the yield and composition of bio-oil. Fuel. 2011;90(9):2915–22. https://doi.org/10.1016/j.fuel.2011.04.033.
6. Wang S, Wang Q, Hu YM, Xu SN, He ZX, Ji HS. Study on the synergistic co-pyrolysis behaviors of mixed rice husk and two types of seaweed by a combined TG-FTIR technique. J Anal Appl Pyrol. 2015;114:109–18. https://doi.org/10.1016/j.jaap.2015.05.008.
7. Hua MY, Li BX. Co-pyrolysis characteristics of the sugarcane bagasse and Enteromorpha prolifera. Energy Convers Manage. 2016;120:238–46. https://doi.org/10.1016/j.enconman.2016.04.072.
8. Li S, Chen X, Liu A, Wang L, Yu G. Study on co-pyrolysis characteristics of rice straw and Shenfu bituminous coal blends in a fixed bed reactor. Biores Technol. 2014;155(2):252–7. https://doi.org/10.1016/j.biortech.2013.12.119.
9. Alvarez J, Amutio M, Lopez G, Bilbao J, Olazar M. Fast co-pyrolysis of sewage sludge and lignocellulosic biomass in a conical spouted bed reactor. Fuel. 2015;159:810–8. https://doi.org/10.1016/j.fuel.2015.07.039.
10. Chiaramonti D, Prussi M, Buffi M, Rizzo AM, Pari L. Review and experimental study on pyrolysis and hydrothermal liquefaction of microalgae for biofuel production. Appl Energy. 2016;185(2):963–72. https://doi.org/10.1016/j.apenergy.2015.12.001.
11. Bu Q, Lei H, Qian M, Yadavalli G. A thermal behavior and kinetics study of the catalytic pyrolysis of lignin. RSC Adv. 2016;6(103):100700–7. https://doi.org/10.1039/C6RA22967K.
12. Deka K, Nath N, Saikia BK, Deb P. Kinetic analysis of ceria nanoparticle catalysed efficient biomass pyrolysis for obtaining high-quality bio-oil. J Therm Anal Calorim. 2017;130(3):1875–83. https://doi.org/10.1007/s10973-017-6476-0.
13. Zhang H, Cheng Y-T, Vispute TP, Xiao R, Huber GW. Catalytic conversion of biomass-derived feedstocks into olefins and aromatics with ZSM-5: the hydrogen to carbon effective ratio. Energy Environ Sci. 2011;4(6):2297. https://doi.org/10.1039/c1ee01230d.
14. Wang D, Xiao R, Zhang H, He G. Comparison of catalytic pyrolysis of biomass with MCM-41 and CaO catalysts by using TGA–FTIR analysis. J Anal Appl Pyrol. 2010;89(2):171–7. https://doi.org/10.1016/j.jaap.2010.07.008.
15. Gao L, Sun J, Xu W, Xiao G. Catalytic pyrolysis of natural algae over Mg-Al layered double oxides/ZSM-5 (MgAl-LDO/ZSM-5) for producing bio-oil with low nitrogen content. Bioresour Technol. 2017;225:293–8. https://doi.org/10.1016/j.biortech.2016.11.077.
16. Wang S, Zhou Y, Liang T, Guo X. Catalytic pyrolysis of mannose as a model compound of hemicellulose over zeolites. Biomass Bioenerg. 2013;57:106–12. https://doi.org/10.1016/j.biombioe.2013.08.003.
17. Wang S, Dai G, Yang H, Luo Z. Lignocellulosic biomass pyrolysis mechanism: a state-of-the-art review. Prog Energy Combust Sci. 2017;62:33–86. https://doi.org/10.1016/j.pecs.2017.05.004.
18. Wang J, Zhong Z, Song Z, Ding K, Deng A. Modification and regeneration of HZSM-5 catalyst in microwave assisted catalytic fast pyrolysis of mushroom waste. Energy Convers Manag. 2016;123:29–34. https://doi.org/10.1016/j.enconman.2016.06.024.
19. Lorenzetti C, Conti R, Fabbri D, Yanik J. A comparative study on the catalytic effect of H-ZSM5 on upgrading of pyrolysis vapors derived from lignocellulosic and proteinaceous biomass. Fuel. 2016;166:446–52. https://doi.org/10.1016/j.fuel.2015.10.051.
20. Zheng A, Zhao Z, Chang S, Huang Z, Wu H, Wang X, et al. Effect of crystal size of ZSM-5 on the aromatic yield and selectivity from catalytic fast pyrolysis of biomass. J Mol Catal

A: Chem. 2014;383–384(3):23–30. https://doi.org/10.1016/j.molcata.2013.11.005.
21. Wang S, Hu Y, Wang Q, Xu S, Lin X, Ji H, et al. TG–FTIR–MS analysis of the pyrolysis of blended seaweed and rice husk. J Therm Anal Calorim. 2016;126(3):1689–702. https://doi.org/10.1007/s10973-016-5762-6.
22. Wang S, Jiang XM, Han XX, Wang H. Fusion characteristic study on seaweed biomass ash. Energy Fuels. 2008;22(4):2229–35. https://doi.org/10.1021/ef800128k.
23. Yildiz G, Ronsse F, Venderbosch R, Duren RV, Kersten SRA, Prins W. Effect of biomass ash in catalytic fast pyrolysis of pine wood. Appl Catal B. 2015;168-169:203–11. https://doi.org/10.1016/j.apcatb.2014.12.044.
24. Yang W, Li X, Li Z, Tong C, Feng L. Understanding low-lipid algae hydrothermal liquefaction characteristics and pathways through hydrothermal liquefaction of algal major components: crude polysaccharides, crude proteins and their binary mixtures. Biores Technol. 2015;196:99–108. https://doi.org/10.1016/j.biortech.2015.07.020.
25. Wang S, Guo X, Wang K, Luo Z. Influence of the interaction of components on the pyrolysis behavior of biomass. J Anal Appl Pyrol. 2011;91(1):183–9. https://doi.org/10.1016/j.jaap.2011.02.006.
26. Wang S, Wang K, Liu Q, Gu Y, Luo Z, Cen K, et al. Comparison of the pyrolysis behavior of lignins from different tree species. Biotechnol Adv. 2009;27(5):562–7. https://doi.org/10.1016/j.biotechadv.2009.04.010.
27. Patwardhan PR, Satrio JA, Brown RC, Shanks BH. Influence of inorganic salts on the primary pyrolysis products of cellulose. Biores Technol. 2010;101(12):4646–55. https://doi.org/10.1016/j.biortech.2010.01.112.
28. Kozłowski M. XPS study of reductively and non-reductively modified coals. Fuel. 2004;83(3):259–65. https://doi.org/10.1016/j.fuel.2003.08.004.
29. Levi G, Senneca O, Causà M, Salatino P, Lacovig P, Lizzit S. Probing the chemical nature of surface oxides during coal char oxidation by high-resolution XPS. Carbon. 2015;90:181–96. https://doi.org/10.1016/j.carbon.2015.04.003.
30. Oliveira RC, Hammer P, Guibal E, Taulemesse J-M, Garcia O. Characterization of metal–biomass interactions in the lanthanum(III) biosorption on Sargassum sp. using SEM/EDX, FTIR, and XPS: preliminary studies. Chem Eng J. 2014;239:381–91. https://doi.org/10.1016/j.cej.2013.11.042.
31. Chen W, Yang H, Chen Y, Xia M, Yang Z, Wang X, et al. Algae pyrolytic poly-generation: influence of component difference and temperature on products characteristics. Energy. 2017;131:1–12. https://doi.org/10.1016/j.energy.2017.05.019.
32. Chen W, Chen Y, Yang H, Xia M, Li K, Chen X, et al. Co-pyrolysis of lignocellulosic biomass and microalgae: products characteristics and interaction effect. Bioresour Technol. 2017;245(Pt A):860–8. https://doi.org/10.1016/j.biortech.2017.09.022.
33. Wang S, Luo Z. Pyrolysis of biomass. Beijing: Science Press; 2016.
34. Chang HK, Park SH, Jeon JK, Dong JS, Jeong KE, Park YK. Upgrading of biofuel by the catalytic deoxygenation of biomass. Korean J Chem Eng. 2012;29(12):1657–65. https://doi.org/10.1007/s11814-012-0199-5.
35. Kabir G, Hameed BH. Recent progress on catalytic pyrolysis of lignocellulosic biomass to high-grade bio-oil and bio-chemicals. Renew Sustain Energy Rev. 2017;70:945–67. https://doi.org/10.1016/j.rser.2016.12.001.